Nuclear- and Radiochemistry

Volume 2: Modern Applications

Edited by
Frank Rösch

DE GRUYTER

Editor
Prof. Dr. Frank Rösch
Universität Mainz
Institut für Kernchemie
Fritz-Strassmann-Weg 2
55128 Mainz, Germany
E-mail: frank.roesch@uni-mainz.de

ISBN 978-3-11-022185-5
e-ISBN (PDF) 978-3-11-022186-2
e-ISBN (EPUB) 978-3-11-039049-0

Library of Congress Cataloging-in-Publication Data
A CIP catalog record for this book has been applied for at the Library of Congress.

Bibliographic information published by the Deutsche Nationalbibliothek
The Deutsche Nationalbibliothek lists this publication in the Deutsche Nationalbibliografie; detailed bibliographic data are available on the Internet at http://dnb.dnb.de.

Cover image: ■
Typesetting: PTP-Berlin, Protago-TEX-Production GmbH, Berlin
Printing and binding: CPI books GmbH, Leck
♾ Printed on acid-free paper
Printed in Germany

www.degruyter.com

Heinz Gäggeler and Sönke Szidat

5 Nuclear dating

Aim: To understand the past is instrumental for predicting the future. Therefore, dating of objects – be they from human activities or from nature – is of prime interest in science. Radionuclides are the most useful tool to tackle this problem. Their half-lives may be used as a clock to measure elapsed time. However, a number of conditions have to be met for proper application of such dating methods. Our environment is rich in radionuclides, mostly of natural origin but partly also from anthropogenic sources such as nuclear weapons testing or from nuclear accidents. This chapter summarizes applications of such radionuclides for dating purpose.

Special emphasis is given to radiocarbon, ^{14}C. For many applications this radioisotope of carbon is the most important dating radionuclide that enables to cover time horizons from the present until about 60 000 years ago. The use of parent/daughter systems is described as well.

Two other short sections address dating via stored signals in the samples from radioactive transformation. These are fission track and thermoluminescence dating.

5.1 Introduction

Knowledge on the age of important objects e.g. of archeological or geological origin, environmental archives, or of our Earth and the solar system or even an object from space such as meteorites, is of great interest to mankind. This interest is based on the public understanding that present and future development can only be understood on the basis of historic information.

Until the discovery of radioactivity in 1896 by Becquerel it was essentially impossible to tackle this problem accurately except in cases where historic documentation was accessible (e.g., debris from documented volcanic eruptions stored in environmental archives such as lake sediments or glacier ice cores). Another example is seasonal information preserved e.g. in accurately documented tree rings. Radioactive transformation of nuclides contained in our environment paved the way to solve many of the most challenging questions about the history and birth or death of many important samples or to study climate variability in the past.

The basis of nuclear dating lies in the fact that the number of atoms $\acute{N}$ of a given radionuclide is correlated with time according to the well-known exponential transformation law,

$$\acute{N}_1 = \acute{N}_0 \exp\{-\lambda (t_0 - t_1)\}, \tag{5.1}$$

where $\acute{N}_1$ and $\acute{N}_0$ denote the number of atoms at time of measurement (t_1) and at time zero (t_0), respectively.

This equation may be transformed into

$$t_0 - t_1 = \Delta t = \frac{1}{\lambda} \ln (\acute{N}_0/\acute{N}_1) , \tag{5.2}$$

which yields the age Δt.

The transformation of a given radionuclide is essentially not altered by environmental influences such as chemical speciation, temperature, pressure or other physical parameters. The transformation constant λ therefore acts as an absolute clock.[1] Radioactivity $\acute{A}$ may be quantified either by measuring the radioactive transformation rate (radiometric method, cf. Chapter 1) or by determining the mass of the nuclide of interest (mass spectrometry, cf. Chapter 4) to obtain the number of atoms. Both quantities are correlated via

$$\acute{A} = \lambda \acute{N} . \tag{5.3}$$

As a rule of thumb, for short-lived radionuclides with half-lives lower than about 100 years it is advisable to perform a radiometric analysis and for nuclides with longer half-lives a mass spectrometric determination. The reason for this time limit is the achieved sensitivity: for short-lived radionuclides a large part of the ensemble of atoms transforms during the measuring time, say a few days at most. This yields an accurate determination of the activity because radiometric analysis may be performed with very high counting efficiency. For longer-lived nuclides the sensitivity of a mass spectrometric analysis becomes superior. Often, accelerator mass spectrometry (AMS) is used for the determination of the number of atoms.[2] This technique may reach overall efficiencies of a few percent and has the great advantage of being essentially background-free. Moreover, AMS enables counting of single separated ions with a counter placed in the focal plane, while conventional mass spectrometers determine separated ions via electric current measurement. This latter technique is not applicable to detection of only few ions. AMS has revolutionized dating with e.g. the radionuclide ^{14}C ("radiocarbon", see below).

In principle four situations exist that are commonly applied in nuclear dating, cf. Tab. 5.1.

The following figures illustrate the four cases using baskets filled with sand where every sand corn represents one atom.

1 Except radionuclides transforming by electron capture, i.e. atoms that undergo a nuclear transformation via capture of an atomic electron. Such a process is slightly influenced by the chemical environment, cf. Chapters 7 and 11 of Vol. I. One example that has been studied in detail is the influence of chemical composition on the transformation of ^{7}Be, a radionuclide quite abundant in the atmosphere. This influence is even larger for nuclei traveling in space. Due to their high velocity such atoms are highly stripped, meaning that they exist only in form of highly positively charged ions with very few if any electrons. Clearly, this influences the probability to capture an atomic electron by the nucleus and changes the radioactive transformation probability significantly.

2 Cf. Chapter 4 on Radionuclide Mass Spectrometry.

Tab. 5.1: Principle situations commonly applied in nuclear dating.

Approach	Example radionuclide	Example application
Transformation from an equilibrium situation	^{14}C	radiocarbon dating
Accumulation of a daughter nuclide	^{222}Rn	dating applied in hydrology
Transformation from a single event injected into the environment	^{3}H	dating of ice cores with maximum deposition in the years 1962–1963 from nuclear weapons testing
Exposure age dating	^{10}Be	age determination of surface rocks

5.1.1 Equilibrium situation

In the equilibrium situation a basket is continuously filled with sand while, simultaneously, the basket loses sand corns (resembling atoms) via a leak at a rate that corresponds to the filling rate (see Fig. 5.1). Therefore, the sand level in the basket is constant (equilibrium level). If, at a given time, the supply of sand is stopped, meaning that the object is disconnected from the continuous supply, the level of sand starts to lower according to the leaking rate. This leaking rate resembles the transformation constant λ of the radionuclide. From knowing the equilibrium level at time zero (t_0) and the level at present time (t_1) the elapsed time Δt since the disconnection from supply can be determined using eq. (5.2). Here, $\acute{N}_0$ means the number of sand corns, i.e. the number of atoms of the radionuclide during the equilibrium situation and $\acute{N}_1$ the present number. A typical example of such a situation is radiocarbon dating.

5.1.2 Accumulation dating

The situation for accumulation dating is depicted in Fig. 5.2. Two baskets are connected via a tube. At time zero basket two is empty (or has a known level). As time elapses, basket one is leaking at a constant rate, resembling the transformation constant of the radionuclides contained in basket one. This leads to a gradual filling of basket two. Hence, with this method, the leaking time is determined from the measured accumulation in basket two at present – if needed corrected for the level at time zero – divided by the leak rate from basket one. This type of dating is frequently used in geology, e.g. using the $^{40}K\,|\,^{40}Ar$ method. In special cases, basket number 2 may also leak, because the species accumulated in basket two is not stable but radioactive. Such a case is the ^{222}Rn dating applied in hydrology.

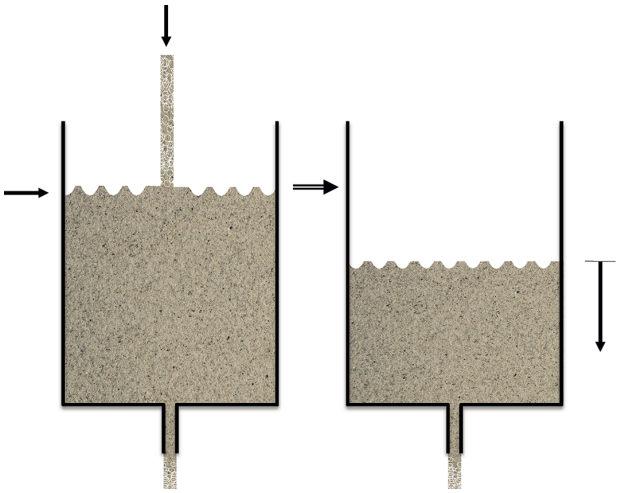

Fig. 5.1: Dating from an equilibrium state. Left side: equilibrium situation at time zero, t_0. The radionuclide is constantly produced at a rate which is equal to the transformation (i.e. loss) rate. Right side: situation at "present time". The radionuclide is no longer produced and transforms according by its half-life.

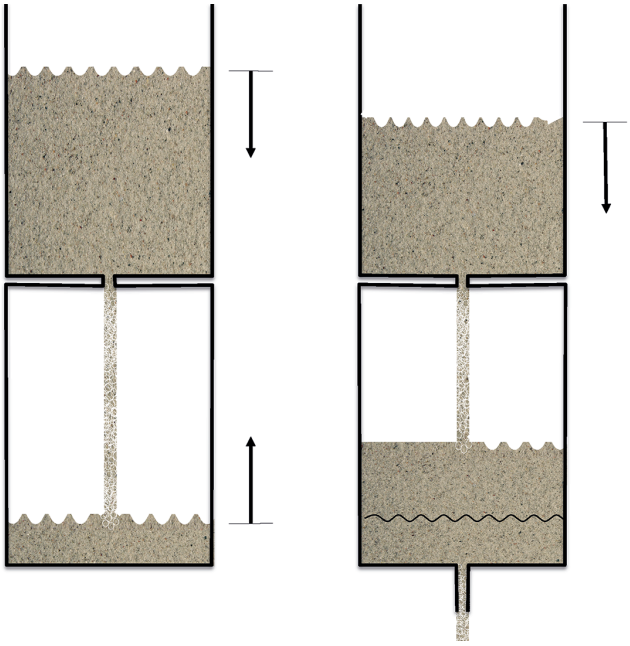

Fig. 5.2: Accumulation dating. Left side: at time zero (t_0) the lower basket has zero or a known filling. Right side: at "present time" the lower basket is partly filled due to transformation from the upper basket. It is possible that also the lower basket has a "leak", i.e. is radioactive.

5.1.3 Decay from a single event

Decay from a single event means that due to an "injection" of a radioactive species into the environment, some compartments, e.g. the atmosphere, have been enriched with this radionuclide. By measuring the radioactivity at present and knowing the activity at time of injection, the elapsed time may be deduced. This situation is reflected in Fig. 5.3. A typical example for this situation is tritium dating using the well-known release ("injection") of this radionuclide into the stratosphere by nuclear weapons testing in the early 1960s.

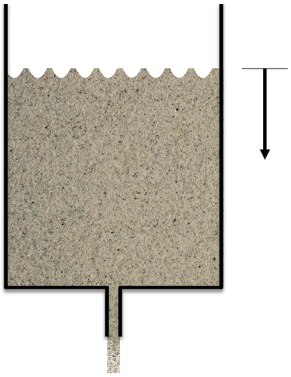

Fig. 5.3: Decay of a radionuclide injected into the environment.

5.1.4 Exposure age

Finally, exposure age dating uses the fact that radioactive nuclides are formed in samples from the Earth's surface because they are exposed to high-energetic primary and secondary cosmic ray particles.[3] Cosmic rays in space are predominantly protons that travel with very high velocities, i.e. high energies. Such cosmic rays and secondary particles (neutrons or myons) formed via interaction with the atmosphere – mainly nitrogen, oxygen and argon – may interact at the Earth's surface with rocks or soil. As a consequence, radioactive nuclides are formed. This means that from the measured amount of such produced radionuclides in the sample and assuming that the amount was zero at time zero (i.e. at a time where the surface was not yet exposed to cosmic rays but covered by a layer of e.g. soil or ice), the time interval since removal of the cover layer may be deduced. This situation is presented in Fig. 5.4. A typical example is exposure age determination of surface rocks by measuring ^{10}Be or ^{26}Al.

3 Cf. Chapter 2 for the origin and impact of cosmic rays.

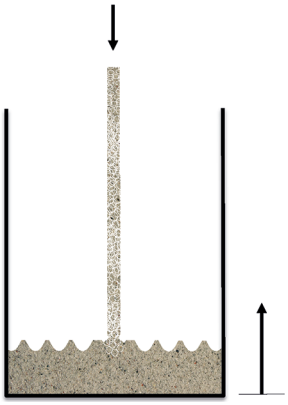

Fig. 5.4: Exposure age dating. At time zero (t_0) production of a radionuclide in the sample starts from zero.

5.1.5 Basic assumptions relevant in nuclear dating

All nuclear dating applications are based on the assumptions listed in Tab. 5.2.

Tab. 5.2: Basic assumptions relevant in nuclear dating.

1	The number of atoms at time zero, $\acute{N}_0$, must be known.	Quite often this prerequisite is not fully met. An example is ^{210}Pb dating. Usually, the equilibrium situation in the past is assumed to be reflected in constant activity concentration in precipitation or the deposition rate of ^{210}Pb per year at a given site to be constant (see text).
2	The system to be dated must be closed.	This means no physical or (geo)chemical processes have changed the sample in such a way that the radionuclide used for dating has been subjected to such processes.
3	The source of the sample is well defined.	Especially in hydrology, water samples quite often represent mixed sources. Such a situation may yield wrong average ages, especially if only one radionuclide is used for dating. Similarly, exposure age determinations with additional surface erosion of the samples may falsify the result.

Let us finally briefly touch on the reliability of a determined age with a given technique, being it radiometric or via mass spectrometry. Two terms are usually used to quantify the quality of the result: *accuracy* and *precision*. Accuracy describes the degree of agreement between measured and true age of a sample, while precision describes the statistical uncertainty of a measurement, usually defined by the number of detected events or atoms.

5.2 Environmental radionuclides

Nuclear dating uses radionuclides from our environment. Figure 5.5 depicts all classes of "environmental radionuclides" plotted with their half-life against the mass number of the nuclides. Only those radionuclides are identified with symbols that are relevant for nuclear dating application. They may be classified according to their origin, cf. Tab. 5.3.

Of primordial origin are those radionuclides that were formed in space and partly survived since the birth of our solar system $4.55 \cdot 10^9$ years ago.

Radiogenic radionuclides are members of the natural transformation chains, hence rather short-lived radionuclides compared to the age of the Earth. They are constantly formed via radioactive transformation of the primordial radionuclides, ^{235,238}U and ^{232}Th, respectively.

Cosmogenic radionuclides are formed by interaction of primary (mostly protons) or secondary (mostly neutrons or myons) particles in the upper atmosphere or on the Earth's surface.

Fission nuclides are formed in nuclear fission processes, mostly of anthropogenic origin. This includes nuclear reactors as well as debris from nuclear weapons testing. In ultratrace amounts, natural fission products also exist on Earth formed via interaction of neutrons with natural uranium or from spontaneous fission of ^{238}U.

Activation products are formed mainly at nuclear facilities via interaction of emitted particles such as neutrons with stable nuclides in close vicinity. An example is

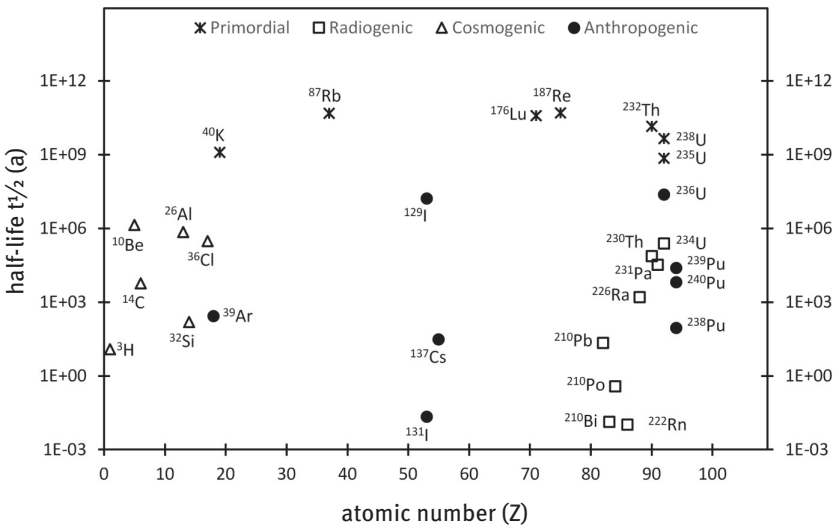

Fig. 5.5: Radionuclides in the environment of different origin as a function of their half-life.

Tab. 5.3: Environmental radionuclides classified by origin.

Origin	Explanation	Examples
Primordial	Produced during element synthesis in our galaxy but having sufficiently long half-lives to still exist in part now	Actinides in nature: ^{235,238}U, ^{232}Th
Radiogenic	Formed in radioactive transformation of primordial radionuclides	^{226}Ra, ^{210}Pb
Cosmogenic	Produced in the interaction of high-energy cosmic ray particles (e.g. protons) with atmospheric constituents (e.g. nitrogen)	^{14}C, ^{10}Be
Fission	Formed in spontaneous fission of actinide nuclides, released by nuclear facilities or in nuclear bombs	^{137}Cs, ^{131}I
Activation	Produced in nuclear reactions with particles (mostly neutrons) emitted in nuclear power plants	^{14}C
Breeding	Formed in nuclear reactions (e.g. with neutrons or heavy ion particles) with actinides	Plutonium isotopes

radiocarbon, formed from atmospheric nitrogen by interaction with neutrons emitted from nuclear reactors in the ^{14}N(n,p)^{14}C reaction.

Breeding means that radionuclides which are not abundant in nature, i.e. isotopes of all elements with atomic numbers higher than 92 (uranium) are formed in nuclear reactions. Artificial radioelements currently exist up to atomic number 118.[4] Some of those radionuclides are also formed in nuclear explosions and have thus been distributed globally, such as the plutonium isotopes ^{239}Pu and ^{240}Pu, respectively. Another isotope of plutonium, ^{238}Pu is frequently used for electric supply in satellites. By accidental failure of a few satellites, ^{238}Pu has been deposited on the Earth's surface at the site of impact.

5.3 Dating with a single radionuclide

Most applications based on the detection of one radionuclide rely on the equilibrium situation, see Fig. 5.1. By some mechanism the radionuclide of interest is formed at a constant rate or at least at a documented rate during the time interval to be dated. This enables a determination of the number of atoms or of the activity at time zero, i.e. $\acute{N}_0$ or $\acute{A}_0$, respectively. A special case is exposure age dating. Here, the radionuclide has zero concentration at time zero and is then formed when the object to be dated is exposed to cosmic rays. A summary of radionuclides discussed in this chapter is compiled in Tab. 5.4.

4 Cf. Chapter 9

Tab. 5.4: Dating with a single radionuclide.

Radionuclide	Half-life in years	Typical application
^{14}C	5730	Dating of carbon containing objects over 60 000 years
^{210}Pb	22.3	Accumulation rate determination of lake sediments, or ice cores over two centuries
^{32}Si	≈ 140	Accumulation rate determination of sediment cores or ice cores over about one millennium
^{10}Be	$1.5 \cdot 10^6$	Accumulation rates of rocks; indirect dating of archives based on chronology of solar activity
^{26}Al	$7.1 \cdot 10^5$	Accumulation rates of rocks
^{36}Cl	$3 \cdot 10^5$	Dating of archives over about one million years; dating of modern archives based on ^{36}Cl injection by nuclear weapons testing

5.3.1 ^{14}C (radiocarbon) ($t_{1/2}$ = 5730 years)

Radiocarbon is a cosmogenic radionuclide. As shown in Fig. 5.6, it is mainly produced in the upper stratosphere by interaction of thermal neutrons formed as secondary particles from primary cosmic rays (mostly protons) with nitrogen according to the nuclear reaction $^{14}N(n,p)^{14}C$. The ^{14}C atoms are instantaneously oxidized to ^{14}CO and in a slower process to $^{14}CO_2$. Due to long residence times of CO_2 in the stratosphere and a slow exchange rate between stratosphere and troposphere, latitudinal differences of ^{14}C production are balanced. This results in a practically constant supply of $^{14}CO_2$ to the troposphere. Again, long residence times lead to a complete spatial mixing of $^{14}CO_2$ in the troposphere within each of both hemispheres, before it is transferred to the biosphere by photosynthesis or to the marine hydrosphere by bicarbonate dissolution. Consequently, living plants and higher organisms consuming such plants contain carbon on the contemporary radiocarbon level, cf. Fig. 5.1, left. After their death, "fresh" carbon ^{14}C is no longer taken up so that the radioactive clock "starts ticking" with the half-life of 5730 years, cf. Fig. 5.1, right. This allows dating of organic or carbonaceous material up to 60 000 years.

Although the stability of CO_2 in the atmosphere results in equilibration of spatial ^{14}C activity concentration, residence times are not long enough to eliminate temporal variability of ^{14}C production. Such variability occurs periodically on short to long timescales (i.e., 10 to 10 000 years) and may amount to 0.5 % to more than 10 %, respectively. As explained above, ^{14}C is produced practically exclusively from galactic cosmic rays. Studies of meteoroids revealed that the energy spectrum and the amplitude of the interstellar galactic cosmic rays have been constant over the past million years. Actually, changes in the ^{14}C production rates are caused by two phenomena, the solar cosmic rays and the magnetic field of the Earth. Both components counteract the galactic cosmic ray intensity thus modulating the impact of the latter to the

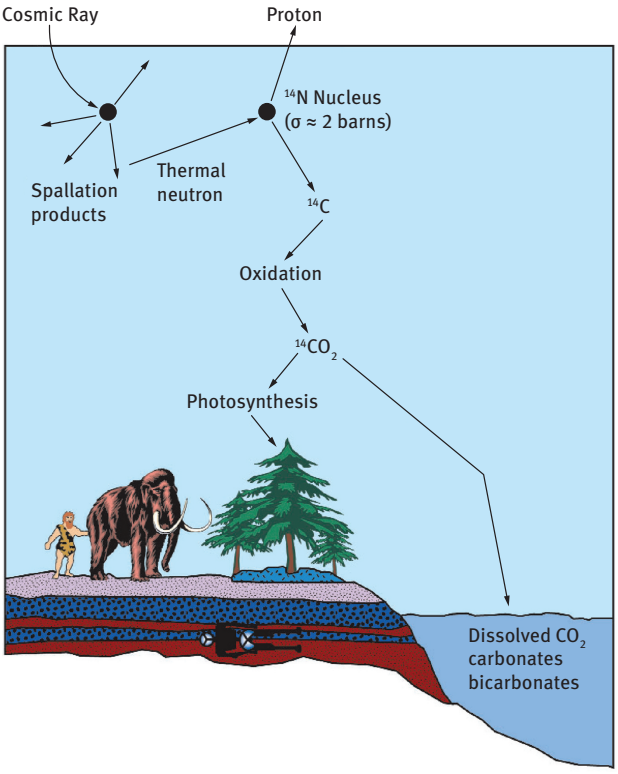

Fig. 5.6: Formation and distribution of natural ^{14}C; adapted from (Currie 2002).

Earth's atmosphere.[5] This leads to decadal up to centennial wiggles, which stem from solar cycles of different frequency.[6] Additional wiggles on timescales of millennia to tens of millennia are caused by changes of the Earth's magnetic field inducing maximum differences of production rates in the order of > 10 %.

In early years of radiocarbon research (i.e. from the 1950s to the 1980s), gas proportional counters (and later liquid scintillator counters, LSC) were employed for measurement of the radioactivity of ^{14}C. Since 1977, accelerator mass spectrometry (AMS) has been increasingly used and has become the main technique for ^{14}C dating today. In

5 A weak sun emitting cosmic rays of reduced fluence on the one hand or a weak magnetic field of the Earth on the other hand (both compared to average conditions) are less able to repel the high-energetic charged particles of intergalactic origin. This results in an enhanced ^{14}C production in the upper stratosphere.

6 The Schwabe cycle with a periodicity of ≈ 11 years leads to an average difference of ^{14}C production between an active and a weak sun of about 5 ‰, whereas the Gleissberg and the DeVries cycles with a periodicity of 90–200 years influence the variability of the radiocarbon production by about 25 ‰, respectively.

AMS, ^{14}C is measured together with the stable carbon isotopes ^{12}C and ^{13}C quasi simultaneously in order to achieve high precision and accuracy of measurement reaching values of 3 ‰ or even better. Consequently, measurement results are given as $^{14}C/^{12}C$ ratios, which are related to the "present" level. The term $F^{14}C$ (fraction of modern radiocarbon) is defined as:

$$F^{14}C = \frac{\left(^{14}C/^{12}C\right)_{sample}}{\left(^{14}C/^{12}C\right)_{modern}} \tag{5.4}$$

Equation (5.4) includes several conventions such as:

1. The year 1950 is considered as the reference year of all radiocarbon measurements thus indicating the "present" or "modern" reference. Therefore, "before present" (often abbreviated as BP) denotes a time before 1950 and "percent modern carbon" (often abbreviated as pMC) indicates the percentage of $(^{14}C/^{12}C)_{sample}$ related to the reference isotopic ratio of modern radiocarbon, i.e. to $100 \cdot F^{14}C$.
2. $(^{14}C/^{12}C)_{modern}$ is defined by convention from reference materials supplied by NIST (National Institute of Standards and Technology from the US Department of Commerce).
3. Isotopic fractionation processes of the three isotopes of carbon may occur either in nature during each chemical or physical transformation within the carbon cycle,[7] in the laboratory during sample pretreatment but also during AMS analysis. In order to correct for such isotopic fractionations, all radiocarbon measurements are related to a reference $^{13}C/^{12}C$ isotopic ratio based on the assumption that fractionations of $^{14}C/^{12}C$ (either in nature or in the laboratory) can be quantified as twice the deviation of the $^{13}C/^{12}C$ ratio from the reference value.

The conventional ^{14}C age Δt is defined as

$$\Delta t = -\ln\left(F^{14}C\right) \cdot 8033 \text{ years}, \tag{5.5}$$

where 8033 years represents the mean lifetime $\tau (= \lambda^{-1} = t_{1/2}/\ln 2)$ based on the "old" ^{14}C half-life of 5568 years as determined in the 1950s. Although the new, correct value is 5730 years, the "old" half-life is still used to guarantee consistency between old published and new data. It therefore follows that the conventional ^{14}C age only reflects a first order estimation of the age of a sample based on the wrong assumption of a constant ^{14}C production and applying an incorrect ^{14}C half-life. The correct ^{14}C age of a sample is then deduced after comparison of the conventional ^{14}C age with a calibration curve. A large effort has been made with radiocarbon analysis of environmental material that was independently dated with other techniques.

7 Every physical or chemical process with carbon-containing compounds leads to a slight but significant change in the isotopic composition of its isotopes (i.e. ^{12}C, ^{13}C, ^{14}C). The reason is the mass dependence of equilibrium constants.

By comparison of the ^{14}C result with the independent (calendar) date, the radiocarbon formation at a given time has been quantified leading to a calibration of the conventional ^{14}C age, Fig. 5.7. Tree rings have been used for the preparation of the calibration curve back to 11 950 BC. The independent dating was performed with dendrochronology. This method enables dating of trees by determination of their ring widths and by combination of overlapping tree-ring chronologies. For the Northern Hemisphere, this technique cannot be continued further back in time due to a lack of suitable trees at the conclusion of the last glacier maximum.

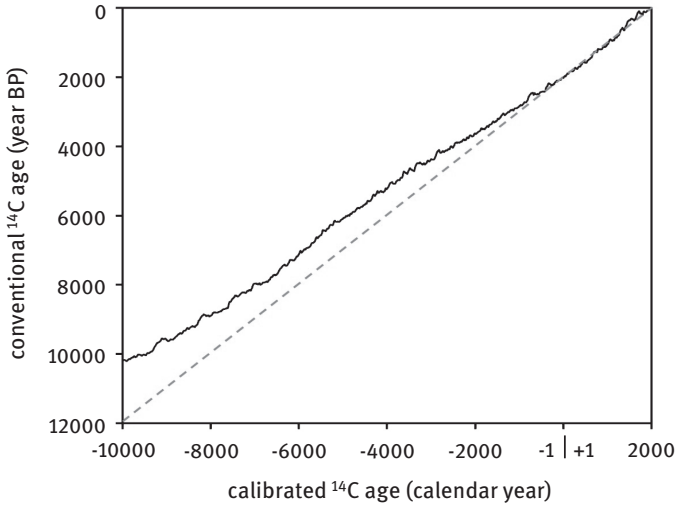

Fig. 5.7: Conventional radiocarbon age in years before present (BP) vs. true age.

In order to continue calibration back to ≈ 60 000 years, other environmental archives have been used such as marine as well as lake sediments, marine corals or speleothems.[8] The independent dating of these samples has been performed with the $^{230}Th|^{234}U$ method (see below) and other approaches, which, however, are less precise than dendrochronology. Calibration of the conventional ^{14}C age of a sample is achieved by convolution of the measurement result with the calibration curve. The calibration procedure increases the dating uncertainties substantially as a consequence of the measurement of the calibration curve itself and of ambiguities of the calibration curve from variable ^{14}C production. Therefore, probability distributions of the calibrated ^{14}C age are not Gaussian – as those of the conventional ^{14}C age are. In some cases, it may be possible that two or even more probable periods for the calibrated date occur with unlikely periods between them. A famous example which

8 Speleothems are stalactites and stalagmites often found in caves.

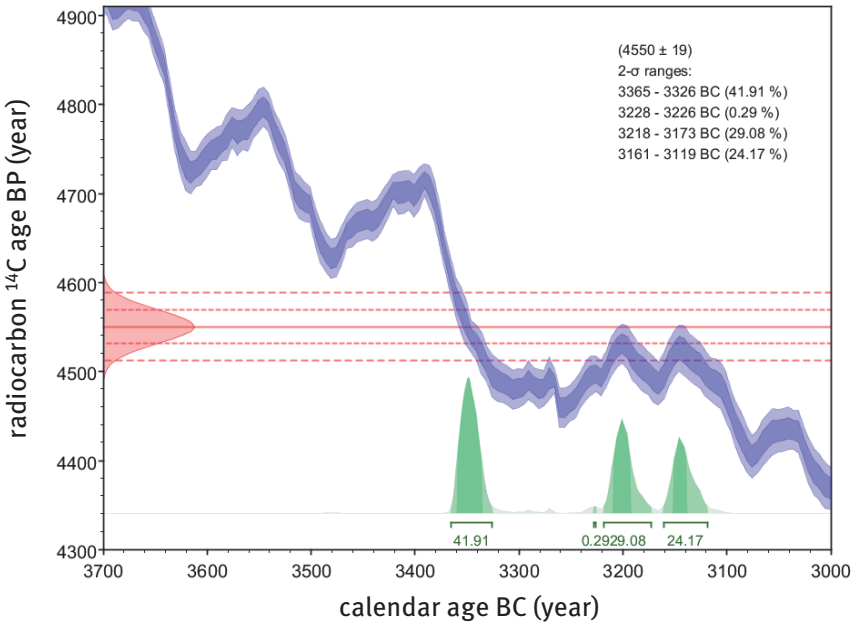

Fig. 5.8: Radiocarbon age in years before present (BP) vs. calibrated age in years before Christ (BC) for the Ötzi iceman. The measured value for the radiocarbon age was 4550 ± 19 years BP (red distribution on *y*-axis). From the calibration curve (blue curve) it follows that within uncertainty several true ages are possible (green probability distributions on *x*-axis) between 3365 BC and 3119 BC; adapted from (Bonani 1994).

yielded unexpected dating uncertainty is the ^{14}C age determination of Ötzi, the iceman found 1991 in the Italian Alps. The ^{14}C measurement resulted in ambiguous solutions for the calibrated date with three possible ages, covering roughly two centuries (see Fig. 5.8).

In many geochemical applications the absolute age of a sample is of minor importance, whereas the deviation of the ^{14}C level compared to the first-order model of constant ^{14}C production is very helpful, as this indicates processes such as the solar and geomagnetic impact on ^{14}C production or reservoir effects. An example is carbon storage in an environmental compartment. For such cases Δ^{14}C is defined as

$$\Delta^{14}\mathrm{C} = \left(F^{14}\mathrm{C} \exp\left[\frac{1950 - t_0}{8267} \right] - 1 \right) \cdot 1000\,‰\,, \tag{5.6}$$

where t_0 is the year of origin of the sample and 8267 represents the mean lifetime in years based on the correct ^{14}C half-life of 5730 years. With the exponential term, a transformation correction is performed according to the age of the sample and based on the assumptions and conditions of eqs. (5.4) and (5.5), respectively. Therefore, all samples meeting these requirements give $\Delta^{14}\mathrm{C} = 0\,‰$ irrespective of their true age of

origin. Positive or negative $\Delta^{14}C$ values indicate deviations of the reference conditions, cf. Fig. 5.9, which may be caused by (a) variability of ^{14}C production, (b) age offsets due to reservoir effects (these additional ages lead only to negative $\Delta^{14}C$ values), or (c) manmade emissions of ^{14}C from surface nuclear bomb explosions or of ^{14}C depleted material from combustion of fossil fuels (which contain no ^{14}C), respectively.

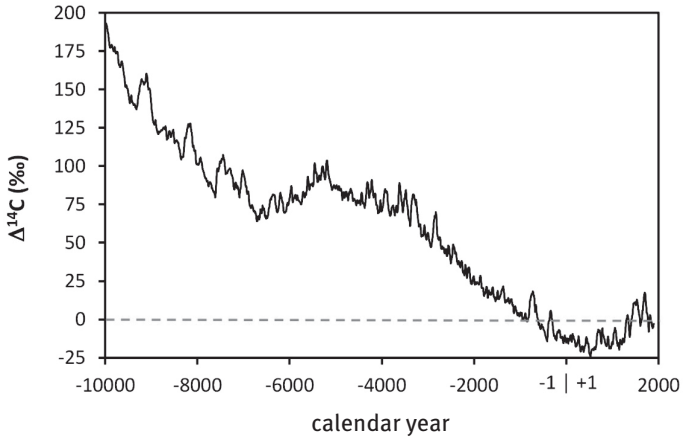

Fig. 5.9: $\Delta^{14}C$ during the last 10 000 years vs. the true age; adapted from (Stuiver 1986).

As already pointed out, ^{14}C can be determined by two fundamentally different techniques. Whereas radiometric techniques such as liquid scintillation or gas proportional counters measure radiocarbon via its radioactive transformation, i.e. $\acute{A}(^{14}C)$ by means of the emitting beta particle, accelerator mass spectrometry (AMS) detects the number $\acute{N}$ of ^{14}C atoms based on mass separation in magnetic and electric fields followed by an energy determination in gas ionization chambers (for details see Chapter 4). This fundamental difference has a substantial effect on the detection efficiencies. For a given number $\acute{N}(^{14}C)$, the efficiency of transformation counting is limited by the ratio of measurement time and half-life of the nuclide. Efficiencies in the order of 10^{-5} are reached for ^{14}C analysis if counting of the samples is restricted to not more than a few days because only very few atoms out of the entire ensemble transform during such a time period. Mass spectrometry of long-lived radionuclides does not depend on this restriction so that only its efficiencies of ionization, transmission and detection are relevant, which can be as high as 10 % for ^{14}C-AMS. This results in a gain in detection efficiency between AMS and radiometric detection by a factor of about 10^4. Consequently, required sample quantities can be reduced from gram amounts for counting techniques to submilligram amounts for AMS, which entails a considerable benefit for dating of valuable samples.

5.3.2 ^{210}Pb ($t_{1/2}$ = 22.3 a)

^{210}Pb is a granddaughter type member of the natural ^{238}U parent transformation series.[9] ^{210}Pb has a half-life of 22.3 years and transforms by β-emission to ^{210}Bi, which has a half-life of 5 days and again transforms via β-emission to ^{210}Po ($t_{1/2}$ = 138.4 d), cf. Fig. 5.10. The β-transformation of ^{210}Pb populates an exited state of the β-emitter ^{210}Bi. This nuclear level de-excites via emission of a γ-ray of 46 keV energy to the ground state. However, this transition is highly converted which means that only in 4 % of transformations is a photon with this energy emitted and in 96 % of transformations an atomic electron. Decay continues then via α-emission with an energy of 5.3 MeV to the stable end product of the ^{238}U transformation series, ^{206}Pb.

The time interval accessible to ^{210}Pb dating is typically one to two centuries at most. It is therefore often applied in studies where environmental archives are investigated covering the industrial time period. Therefore, most applications of this radionuclide intend to study pollution records caused by industrial emissions in appropriate archives (e.g. ice cores) or to determine accumulation rates during the last century in lake sediments.

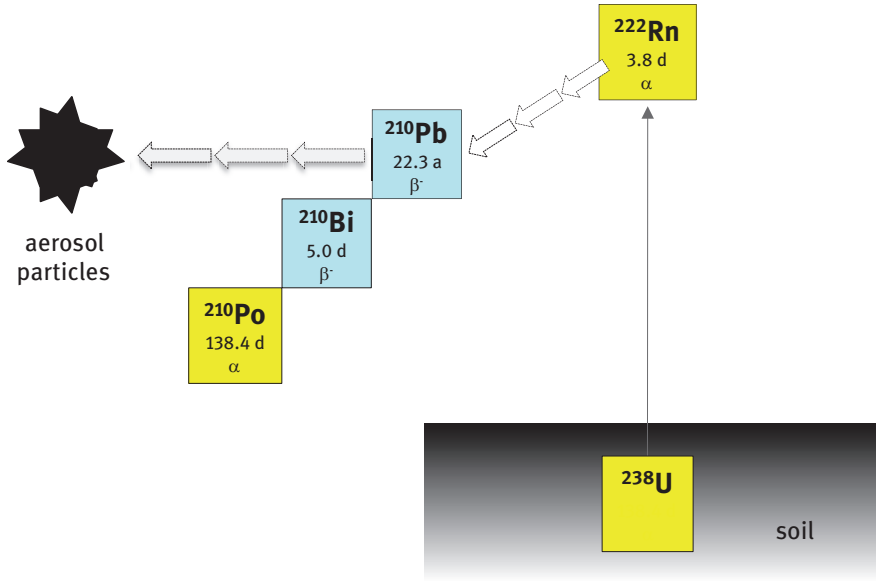

Fig. 5.10: Origin and fate of ^{210}Pb in the atmosphere. ^{222}Rn, formed in soil via transformation of ^{238}U, is emanating into the atmosphere. After further transformation, generated ^{210}Pb attaches to aerosol particles which are scavenged by precipitation and deposition onto to the Earth's surface. ^{210}Pb further transforms via short-lived ^{210}Bi to ^{210}Po and finally to stable ^{206}Pb.

9 Natural series of transformation are discussed in Chapter 3 of Vol. I.

Based on the rather short half-life of ^{210}Pb it is advisable to measure it via radiometric techniques and not via mass spectrometry. Three options exist to determine the ^{210}Pb activity concentration (i) β-counting of ^{210}Pb and/or ^{210}Bi, (ii) γ-counting of ^{210}Pb, and (iii) α-counting of the granddaughter ^{210}Po.

β-counting has not found widespread application, despite being very sensitive and of high precision. The reason is the high radiochemical purity of the sample needed prior to measurement. Since β-counting (e.g. using gas proportional or liquid scintillation counters) is not nuclide-specific, a sophisticated chemical purification of the sample is mandatory to suppress any contamination by the vast amount of environmental radionuclides that also transform via β-emission. Such a separation procedure is very time consuming.

If the sample has a sufficiently high ^{210}Pb activity, γ-counting is the method of choice. This situation is often met when analyzing sediment samples. Unfortunately, for determination of ^{210}Pb in precipitation, the sensitivity achieved in γ-counting is not sufficient for reasonably sized volumes, say 1 liter. In this case, ^{210}Pb is usually determined via detection of ^{210}Po. This method, however, requires secular equilibrium[10] between the three radionuclides ^{210}Pb, ^{210}Bi, and ^{210}Po, respectively. This is reached after about one year. Advantage of this radiometric technique is the high sensitivity because α-counting yields energy-resolved data at a 100 % counting efficiency of the used silicon detectors. The overall efficiency is then only determined by geometrical parameters, i.e. the size of the detector facing the sample.

^{210}Pb dating is frequently applied for lake sediments and glacier ice. Figure 5.11 depicts such a dating of a sediment core from Lake Zürich, Switzerland. Also inserted into the figure are measurements of ^{137}Cs, a radionuclide formed in nuclear fission. This radionuclide was globally distributed from nuclear weapons testing during Soviet Union and USA tests peaking in the years 1962–1963. The ^{210}Pb activity concentrations depicted in Fig. 5.11 are not the total but the so-called "unsupported" activities. Since sediment materials contain ^{238}U, ^{210}Pb is constantly formed via nuclear transformation. This "supported" ^{210}Pb has therefore to be subtracted from the measured total ^{210}Pb activity concentration. This is usually made by measuring the ^{210}Pb activity concentration in very deep samples, which are too old for ^{210}Pb dating. This value is then considered as the "supported" ^{210}Pb activity concentration and is subtracted from all measured values to yield the values for "unsupported" ^{210}Pb. From Fig. 5.11 it is evident that at the surface of the sediment the ^{210}Pb activity concentrations are nearly constant down to a depth of about 1.5 g/cm^2. From the ^{137}Cs measurement this depth can be dated to be roughly 1963. The explanation for this inconsistency between ^{137}Cs and ^{210}Pb data comes from a process often observed in lake sediments: biogenic perturbation (*bioturbation*). Microorganisms are actively mixing organic material until a certain depth, which influences the surface profile of ^{210}Pb. It is interesting to note

10 See Chapter 3 in Vol. I for mathematical aspects of radioactive equilibria.

that ^{137}Cs, which is predominantly attached to clay minerals, is not influenced by this process. The right axis of Fig. 5.11 depicts the combined age information from the ^{137}Cs and the ^{210}Pb measurements. From the age-depth relationship an average annual mass sedimentation rate of about 50 mg/cm^2 can be deduced.

It should be mentioned that analysis of the data depicted in Fig. 5.11 assume a constant initial concentration (CIC model) of unsupported ^{210}Pb. This means that the sediment core is assumed to have a constant sedimentation rate with always the same initial ^{210}Pb activity concentration. If, however, for the time period under study the sedimentation rate changed, then such an assumption is incorrect. It is then advisable to assume constant rate of supply (CRS model), meaning that the annual deposition rate of ^{210}Pb is constant at variable sedimentation rate. As a consequence, for years with lower than average accumulation rates the activity concentrations are higher and vice versa. For a detailed description of ^{210}Pb in sediment dating using the twomodels and a combination of both, see Appleby (2008).

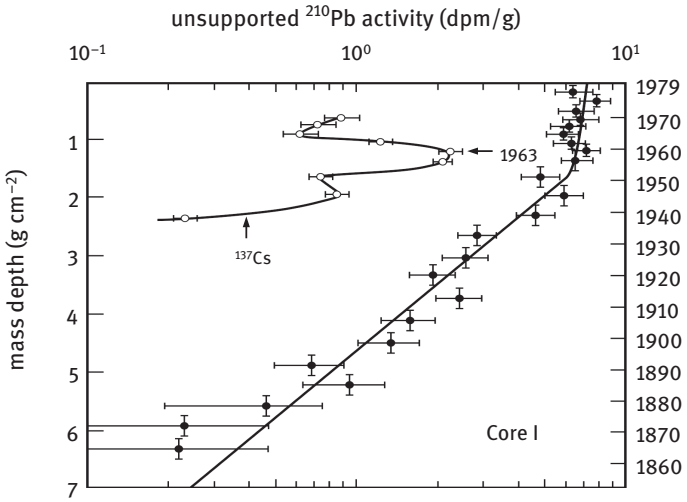

Fig. 5.11: ^{210}Pb activity concentrations as a function of depth for a sediment core from Lake Zürich. Also shown is the activity of ^{137}Cs from nuclear weapons testing (Erten 1995).

Figure 5.12 illustrates the ^{210}Pb activity concentration along an ice core drilled on Colle Gnifetti, Switzerland (saddle at 4450 m above sea level). Since ice contains negligible amounts of mineral dust as a source of "supported" ^{210}Pb, no corrections are needed. Hence, the data shown represent the measured values. From the radioactivity distribution along the ice core the age depicted on the right axis may be deduced.

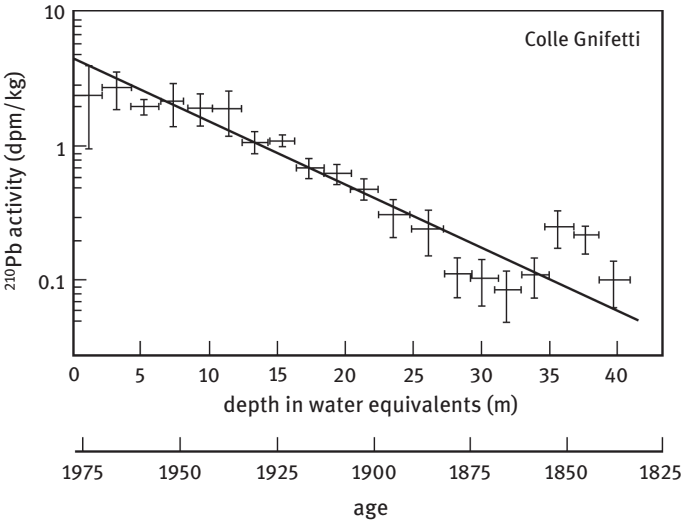

Fig. 5.12: ^{210}Pb activity concentrations along an ice core from the Colle Gnifetti at 4450 m above sea level, Swiss Alps.

5.3.3 ^{32}Si ($t_{1/2} \approx 140$ a)

^{32}Si is produced in the upper atmosphere via interaction of cosmic rays with the argon isotope ^{40}Ar in the spallation reaction ^{40}Ar(p,2αp)^{32}Si. As a nonvolatile product it attaches to aerosol particles and is transported within about one week to the Earth's surface, where it is deposited mostly by wet precipitation.

^{32}Si has a half-life of about 140 years.[11] ^{32}Si would be an ideal tool to date samples in the range between one century and one millennium, hence between the optimum dating ranges of ^{210}Pb and ^{14}C. However, besides the poorly known half-life, there are several drawbacks that have prevented such applications so far. The activity concentration of ^{32}Si in air is very low, because ^{40}Ar is a minor component of ambient air (0.9 %). This means that a radiometric determination of ^{32}Si requires large sample volumes, e.g. about one ton of water. Typical values of ^{32}Si activity concentrations in one ton of precipitation (or snow) are a few mBq only. Therefore, in recent years attempts were made to measure ^{32}Si via AMS. But this approach is also limited due the fact that silicon is very abundant in nature. In environmental samples the ratio between the radioactive isotope ^{32}Si and the stable isotopes of silicon, mainly ^{28}Si with 92.2 %

11 The accuracy of current literature data is still surprisingly poor. The published values range from about 100 to 170 years

abundance, is extremely low. Typical values are between 10^{-15} and 10^{-17}.[12] One of the very few examples where ^{32}Si dating was successfully applied is depicted in Fig. 5.13. It shows the ^{32}Si (and ^{210}Pb) depth profiles of a marine sediment core from Bangladesh. The measurements were performed using radiometric technique by measuring the nuclide ^{32}P with a half-life of 14.3 days in secular equilibrium, a high-energy β-emitter formed in the β-transformation of ^{32}Si. The interpretation of this study yielded a sedimentation rate for the uppermost part of the core (dated with ^{210}Pb) of 3.1 cm per year. Below this surface layer it was much lower, 0.7 cm per year. The proposed interpretation of this significant change in sedimentation rate was that it reflects increased sedimentation loads over the first 50 years due to human activities in this area.

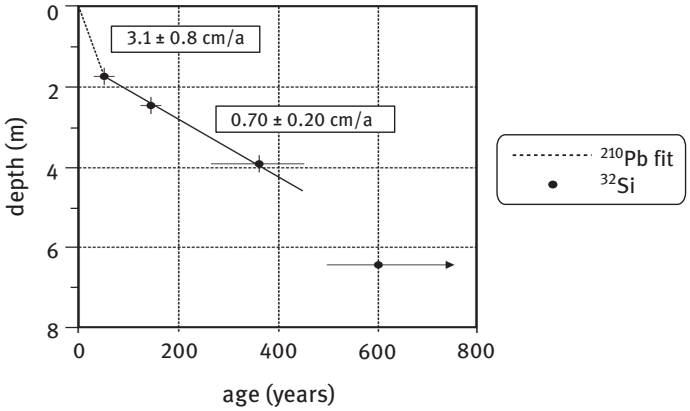

Fig. 5.13: Depth age relationship of a sediment core from Bangladesh deduced from measured ^{210}Pb and ^{32}Si activity concentration; adapted from (Morgenstern 2001).

5.3.4 ^{129}I ($t_{1/2} = 1.6 \cdot 10^7$ a)

In nature two isotopes of iodine exist, ^{127}I which is stable, and the long-lived radioactive ^{129}I. ^{129}I has three different sources, (a) cosmogenic, (b) fissiogenic, and (c) anthropogenic. Cosmogenic ^{129}I is formed in the atmosphere via interaction of cosmic rays with xenon. Fissiogenic ^{129}I is produced via spontaneous fission of ^{238}U contained in the Earth's crust. Finally, nuclear weapons testing emitted ^{129}I in considerable amounts into the atmosphere. More recently, also reprocessing plants emitted ^{129}I into the atmosphere but also into the marine environment. These anthropogenic sources surpass the cosmogenic and fissiogenic sources by far. Usually ^{129}I is de-

12 Since AMS measures the ratio between the radioactive isotope and usually a stable isotope of the same element, a determination of ^{32}Si by this technique is at the cutting edge of AMS technology. Only in very pure samples, e.g. in ice samples from New Zealand glaciers or from Antarctica, has it so far been possible to measure ^{32}Si by AMS.

termined in environmental samples relative to the stable ^{127}I. Ratios are $1.5 \cdot 10^{-12}$ for pre-anthropogenic iodine. This value can be found in oceanic water that has not yet been influenced by anthropogenic input. Rain water in central Europe, however, is much influenced by emissions from the reprocessing plants in Sellafield (Great Britain) and La Hague (France). Typical isotopic ratios may be as high as 10^{-6}.

Application of ^{129}I for dating purpose is mostly in hydrology. Due to the long half-life of ^{129}I reliable dating starts at ages of several million years. This includes age determination of very old aquifers assuming the influence of fissiogenic and anthropogenic ^{129}I to be negligible. Dating based on fissiogenic ^{129}I may be applied for geothermal fluids. In this case, the concentration of ^{238}U must be known as well as the transfer yield of ^{129}I from the ^{238}U source to the fluid. Some applications focus on detection of anthropogenic ^{129}I. In these cases the samples are very young.

In all these applications, ^{129}I is measured with highest sensitivity via AMS, relative to the stable isotope ^{127}I. Some applications applied neutron activation analysis as an analytic tool. Here, ^{129}I is determined via formation of ^{130}I ($t½ = 12.4$ h) after neutron capture at a research reactor.

5.3.5 ^{10}Be ($t½ = 1.5 \cdot 10^6$ a)

^{10}Be is a cosmogenic radionuclide formed in the upper atmosphere predominantly in the spallation reactions between neutrons (secondary cosmic rays) with nitrogen ($^{14}N(n,3p2n)^{10}Be$). This radionuclide has been used to trace variability of solar activity back in time, because solar activity is anti-correlated with galactic cosmic ray intensity (see the section on radiocarbon dating). Ice cores from Antarctica have mostly been used as archives of this solar history. ^{10}Be is incorporated into such ice cores via precipitation. These investigations enabled dating of periods with low solar activity such as the MAUNDER minimum from 1645–1715, which is assumed to be responsible for a climatic depression ("Little Ice Age"). Hence, this dating is based on the "fingerprint" idea: fluctuations of ^{10}Be activity concentrations in the sample over time are compared to known fluctuations of solar variability in the past.

Another fast developing application of ^{10}Be is exposure age determination. This application is based on the fact that the Earth's surface is exposed to cosmic ray bombardment. Though the intensity of this bombardment is very small – due to a high absorption of cosmic rays in the atmosphere – it is still sufficiently intense to form some radionuclides via nuclear reactions, such as ^{10}Be in the reactions $^{16}O(\alpha,2pn)^{10}Be$ or $^{16}O(\mu^-,\alpha pn)^{10}Be$, respectively (see Fig. 5.14).

Therefore, based on known production rates of ^{10}Be in a given geological surface, the exposure age may be determined. However, one drawback in real applications is the erosion rate. If the surface to be dated is significantly influenced by erosion, then the concentration of ^{10}Be levels off after a certain time (see Fig. 5.15). At saturation, production and erosion are in equilibrium and dating is no longer possible.

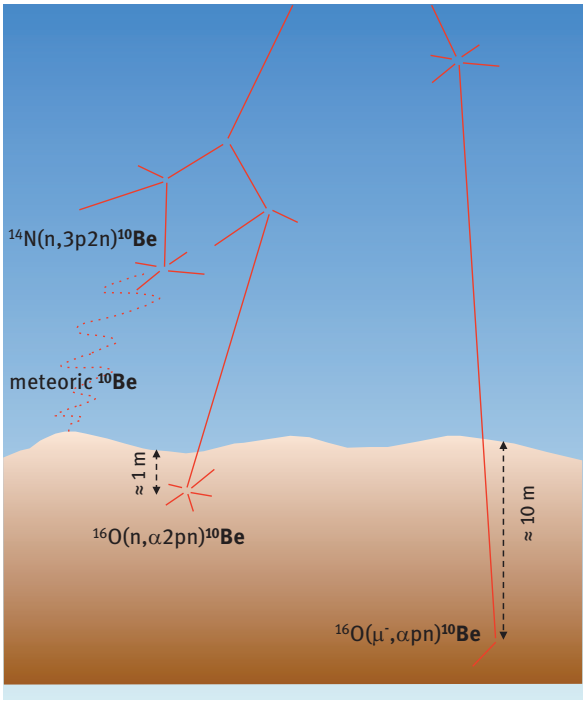

Fig. 5.14: ^{10}Be produced through interaction of secondary cosmic rays (neutrons or myons) with the Earth's surface.

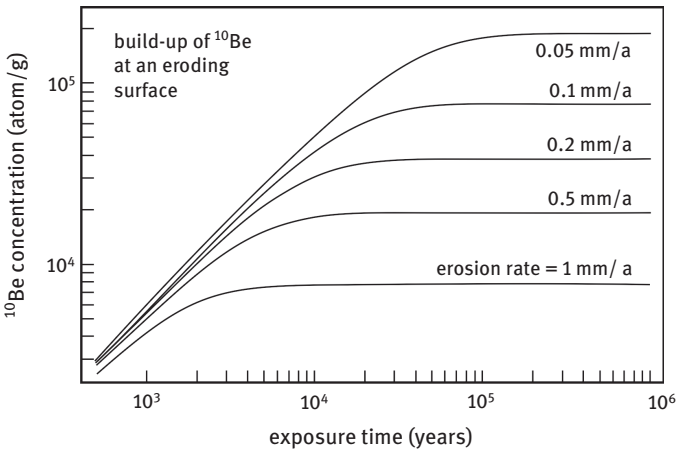

Fig. 5.15: Number of ^{10}Be atoms formed in an exposed surface as a function of time for different values of known surface erosion rates calculated via eq. (5.7).

Measured production rates in surface rock samples from North America yielded about five ^{10}Be atoms produced per gram and year (Balco et al. 2008). To determine the erosion rate, a second radionuclide is required because the influence of erosion on the build-up of radioactive atoms depends on the half-life of the radionuclide. ^{26}Al is mostly used for this purpose (see below).

5.3.6 ^{26}Al ($t_{1/2} = 7.1 \cdot 10^5$ a)

^{26}Al is also a radionuclide formed on the Earth's surface via interaction with cosmic rays in different nuclear reactions, depending on the geological composition, e.g. in ^{28}Si(p,p2n)^{26}Al, or ^{28}Si(μ^-,3n)^{26}Al, respectively. Measured production rates in surface rock samples from North America yielded about thirty ^{26}Al atoms produced per gram and year (Balco et al. 2008).

^{26}Al is often measured together with ^{10}Be using AMS in cases where erosion is assumed to be important. Measured exposure ages reach values of up to one million years (Balco et al. 2008). The exposure age can then be determined from the two radionuclides ^{10}Be and ^{26}Al via:

$$\acute{N}_x = P_{0,x}/\{\lambda_x + \varepsilon_{ero}/a_x\} \tag{5.7}$$

with

$\acute{N}_x$ number of measured atoms of x (^{10}Be or ^{26}Al) in the sample (atoms g^{-1})
$P_{0,x}$ production rate of species x at the surface (atoms g^{-1} a^{-1}); e.g. 5 for ^{10}Be and 30 for ^{26}Al (see above)
λ_x transformation constant of species x (a^{-1})
ε_{ero} erosion rate (g cm^{-2} a^{-1})
a_x effective attenuation depth of spallation product formation for ^{10}Be or ^{26}Al, respectively, in the sample (assumed to be 160 g cm^{-2}).

Hence, eq. (5.7) has two variables, $\acute{N}_x/P_{0,x}$ (which is the exposure age in years) and ε_{ero}, the erosion rate.[13]

5.3.7 ^{36}Cl ($t_{1/2} = 3.0 \cdot 10^5$ a)

^{36}Cl is formed by cosmic rays, mostly in the atmosphere via interaction with argon (^{40}Ar(p,αn)^{36}Cl) but also in nuclear weapons testing. Cosmic ray produced ^{36}Cl has found application as a dating tool for archives up to a few million years. Another

13 The method for dating is available under http://hess.ess.washington.edu.

application is to use anthropogenic ^{36}Cl production via activation of sea-salt particles from the nuclear weapons testing in the Bikini Atoll in the late 1950s (see Fig. 5.21 from Section 5.6) as a dating horizon.

^{36}Cl is measured with highest sensitivity using AMS. Due to strong interference of ^{36}Cl with the isobaric stable isotope of sulfur (^{36}S), ^{36}Cl can only be measured with big AMS accelerators that have a high accelerator voltage of several MV. Under these conditions accelerated ions have high velocities (i.e. high kinetic energies), which enables efficient separation of the isobaric nuclides ^{36}Cl and ^{36}S by a gas-filled magnetic separator coupled to the accelerator.

5.4 Accumulation dating with a radioactive parent and a stable daughter

Most applications of this dating principle are in geochronology and cosmochronology, because the half-lives of the mostly used systems are very long, reaching the age of the solar system. Knowing the actual activity and half-life of the transforming parent nuclide together with the concentration of the daughter nuclide (radioactive or stable) at time zero, the age can be inferred. Table 5.5 summarizes the examples discussed in this chapter.

Tab. 5.5: Parent-daughter dating systems for application in geochronology and cosmochronolgy as well as in hydrology (^{222}Rn | ^{226}Ra).

Mother	Half-life (a)	Daughter	Half-life (a)
^{238}U	$4.468 \cdot 10^9$	^{206}Pb	stable
^{235}U	$7.038 \cdot 10^7$	^{207}Pb	stable
^{232}Th	$1.405 \cdot 10^{10}$	^{208}Pb	stable
^{87}Rb	$4.8 \cdot 10^{10}$	^{87}Sr	stable
^{40}K	$1.28 \cdot 10^9$	^{40}Ar	stable
^{234}U	$2.455 \cdot 10^5$	^{230}Th	$7.54 \cdot 10^5$
^{235}U	$7.038 \cdot 10^7$	^{231}Pa	$3.276 \cdot 10^4$
^{226}Ra	$1.6 \cdot 10^3$	^{222}Rn	3.8 days

The most important examples are the natural transformation series starting with ^{235,238}U and ^{232}Th and ending in the stable isotopes ^{206,207,208}Pb. Moreover, the ^{40}K | ^{40}Ar and ^{87}Rb | ^{87}Sr systems, where radioactive ^{40}K ($t½ = 1.28 \cdot 10^9$ a) or ^{87}Rb ($t½ = 4.8 \cdot 10^{10}$ a) transform into stable ^{40}Ar or ^{87}Sr, respectively, are also widely used. Some other systems of minor importance are ^{187}Re | ^{187}Os (^{187}Re: $t½ = 4.1 \cdot 10^{10}$ a), ^{176}Lu | ^{176}Hf (^{176}Lu: $t½ = 3.6 \cdot 10^{10}$ a), or ^{40}K | ^{40}Ca, which takes into account that 11 % of ^{40}K transforms into ^{40}Ar (see above) while 89 % transforms into ^{40}Ca.

Let us denote the number of radioactive parent nuclides with $\acute{N}^{p}$ and the number of stable daughter nuclei with $\acute{N}^{d}$. Then the time dependence of the number of parent nuclei at time t is:

$$\acute{N}^{p}(t) = \acute{N}^{p}(t_0)\, e^{-\lambda t}\,, \tag{5.8}$$

with t_0 referring to time zero. The number of daughter nuclei at time t is:

$$\acute{N}^{d}(t) = \acute{N}^{d}(t_0) - \left[\acute{N}^{p}(t_0) - \acute{N}^{p}(t)\right]\,. \tag{5.9}$$

Combining eqs. (5.8) and (5.9) leads to eq. (5.10). Equation (5.11) calculates the required parameter: time.

$$\acute{N}^{d}(t) = \acute{N}^{d}(t_0) + \acute{N}^{p}(t)\,(e^{\lambda t} - 1) \tag{5.10}$$

$$t = \frac{1}{\lambda} \ln\left\{1 + \left[(\acute{N}^{d}(t) - \acute{N}^{d}(t_0))/\acute{N}^{p}(t)\right]\right\}\,. \tag{5.11}$$

It requires the measurement of the concentrations of parent and daughter at time t, usually at present. Moreover, some assumptions are needed for the concentration of the daughter at time zero. It should be added that dating requires that the system remained "closed" during the time window to be dated, hence without any geochemical processes that might influence the parent and/or daughter nuclide.

5.4.1 Dating with the natural transformation series

The parent|daughter systems considered are $^{238}U\,|\,^{206}Pb$ ($t_{1/2}{}^{238}U = 4.468 \cdot 10^9$ a), $^{235}U\,|\,^{207}Pb$ ($t_{1/2}{}^{235}U = 7.038 \cdot 10^8$ a), and $^{232}Th\,|\,^{208}Pb$ ($t_{1/2}{}^{232}Th = 1.405 \cdot 10^{10}$ a). It is assumed that the intermediate transformation products between radioactive parent and stable daughter are too short-lived to be of importance for the dating application.[14]Dating with the natural transformation series requires an assumption about the concentration of the terminal daughters (i.e. $^{206,207,208}Pb$) at time zero.[15] For deter-

14 It is interesting to note that the very first application of dating with the natural transformation series was not based on the systems listed above but on the fact that in the transformation series many α-particles are emitted, namely 8 α-particles in the transformation chains of ^{238}U, 7 α-particles of ^{235}U, and 6 α-particles of ^{232}Th, respectively. After having captured two electrons from the surroundings these α-particles become stable helium atoms (^{4}He). This means that the number of helium atoms in a sample is correlated to the age. Based on this principle, Rutherford estimated the age of our Earth from the concentration of helium in uranium ores to be about $0.5 \cdot 10^9$ years. This value turned out to be roughly one order of magnitude too short which was later explained as being caused by partial loss of helium during metamorphosis processes.

15 There is one stable isotope of lead, ^{204}Pb, which is not formed as end product of any natural transformation series. The natural isotopic composition of lead, not influenced by transformation from uranium or thorium (named nonradiogenic composition) is ^{204}Pb: 1.4 %, ^{206}Pb: 24.1 %, ^{207}Pb: 22.1 %, and ^{208}Pb: 52.4 %, respectively. The radiogenic contribution of ^{206}Pb, ^{207}Pb, or ^{208}Pb in an ore can then be determined by measuring the ^{204}Pb concentration and subtracting the nonradiogenic contribution.

mination of the concentration of lead isotopes mostly thermal ionization mass spectrometry (TIMS) is used. When needed, uranium and thorium are measured using high-resolution inductively coupled plasma mass spectrometry (HR-ICP-MS).

In practical applications, usually two of the three transformation chains are combined. This enables to check whether the system under study was indeed closed, hence, has not been subjected to any geological processes that might have led to a loss of lead, which is a volatile element. Such curves are called *concordia*.

Let us consider the two uranium transformation series and define R_6 and R_7 as follows:

$$R_6 = \frac{\acute{N}(^{206}\mathrm{Pb}/^{204}\mathrm{Pb})(t) - \acute{N}(^{206}\mathrm{Pb}/^{204}\mathrm{Pb})(t_0)}{\acute{N}(^{238}\mathrm{U}/^{204}\mathrm{Pb})(t)} \tag{5.12}$$

and

$$R_7 = \frac{\acute{N}(^{207}\mathrm{Pb}/^{204}\mathrm{Pb})(t) - \acute{N}(^{207}\mathrm{Pb}/^{204}\mathrm{Pb})(t_0)}{\acute{N}(^{235}\mathrm{U}/^{204}\mathrm{Pb})(t)} \,. \tag{5.13}$$

Figure 5.16 shows the concordia as a plot of R_6 against R_7. If experimental results lie on the line, then the system was closed. If the values are below the line then this indicates loss of lead or a gain of uranium, and vice versa for data above the line. The numbers listed along the lines represent the age in 10^9 years.

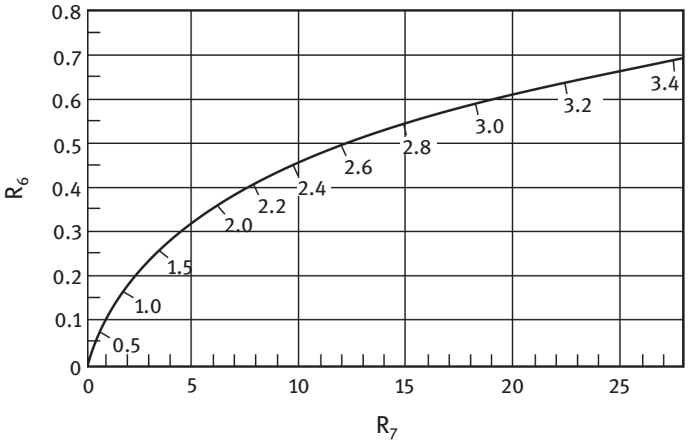

Fig. 5.16: Concordia for R_6 (eq. (5.12)) against R_7 (eq. (5.13)) (Friedländer et al. 1981). The numbers listed along the lines represent the age in 10^9 years.

It is also possible to date solely via the concentration ratio between ^{206}Pb and ^{207}Pb, if the sample contains no natural (nonradiogenic) lead, meaning that the concentration of ^{204}Pb is zero. Taking eq. (5.10) and setting $\acute{N}^{\mathrm{d}}(t_0) = 0$ leads at time t to

$$\acute{N}(^{206}\mathrm{Pb}/^{207}\mathrm{Pb}) = \frac{\acute{N}(^{238}\mathrm{U})\,(\mathrm{e}^{\lambda(^{238}\mathrm{U})t} - 1)}{\acute{N}(^{235}\mathrm{U})\,(\mathrm{e}^{\lambda(^{235}\mathrm{U})t} - 1)} \,. \tag{5.14}$$

With the natural isotopic composition of uranium (^{235}U = 0.72 % and ^{238}U = 99.2745 %, i.e. $\acute{N}(^{238}\mathrm{U})/\acute{N}(^{235}\mathrm{U}) = 137.8$), eq. (5.14) results in:

$$\acute{N}(^{206}\mathrm{Pb}/^{207}\mathrm{Pb}) = 137.8\,\frac{\mathrm{e}^{\lambda(^{238}\mathrm{U})t} - 1}{\mathrm{e}^{\lambda(^{235}\mathrm{U})t} - 1}\,. \tag{5.15}$$

This correlation is depicted in Fig. 5.17.

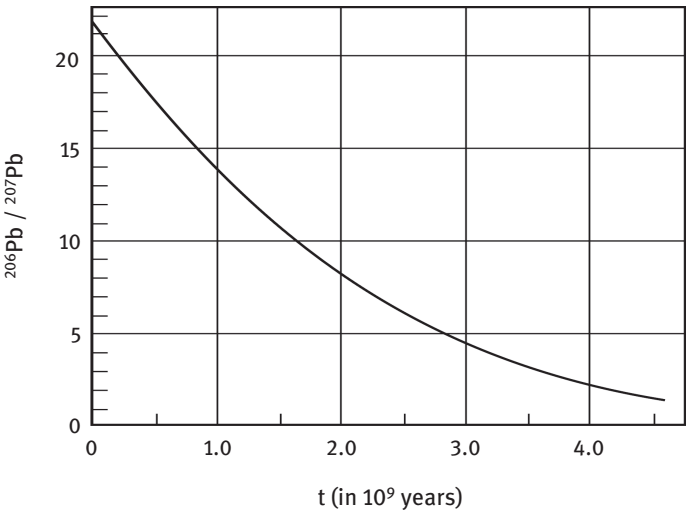

Fig. 5.17: Dating based solely on ^{206}Pb/^{207}Pb for cases where the sample does not contain nonradiogenic lead (Friedländer et al. 1981).

If in a class of samples of identical age, e.g. meteorites of a given type, the concentration of lead isotopes ^{206}Pb and ^{207}Pb are measured relative to the nonradiogenic isotope ^{204}Pb for different subsamples, then a correlation is obtained named an *isochron*.

$$\begin{aligned}\frac{\acute{N}(^{207}\mathrm{Pb}/^{204}\mathrm{Pb})(t) - \acute{N}(^{207}\mathrm{Pb}/^{204}\mathrm{Pb})(t_0)}{\acute{N}(^{206}\mathrm{Pb}/^{204}\mathrm{Pb})(t) - \acute{N}(^{206}\mathrm{Pb}/^{204}\mathrm{Pb})(t_0)} &= \frac{\acute{N}(^{235}\mathrm{U})\,(\mathrm{e}^{\lambda(^{235}\mathrm{U})t} - 1)}{\acute{N}(^{238}\mathrm{U})\,(\mathrm{e}^{\lambda(^{238}\mathrm{U})t} - 1)} \\ &= \frac{1}{137.8}\,\frac{\mathrm{e}^{\lambda(^{235}\mathrm{U})t} - 1}{\mathrm{e}^{\lambda(^{238}\mathrm{U})t} - 1}\,.\end{aligned} \tag{5.16}$$

An example of an isochronous dating for L-chondrites, a class of meteorites, is depicted in Fig. 5.18. All data on the isochronous correlation yield an age of $4.55 \cdot 10^9$ years, which is the age of our solar system.

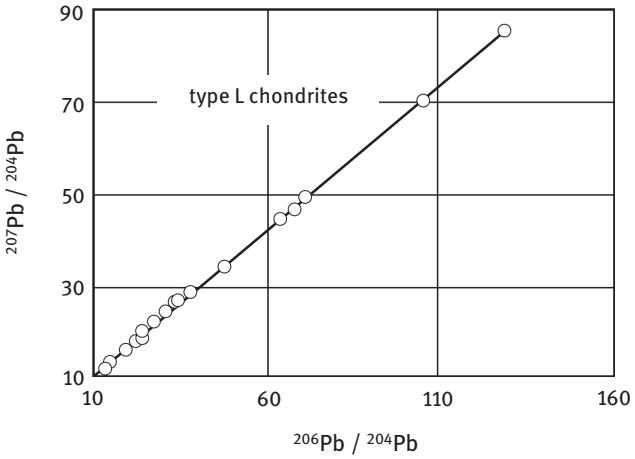

Fig. 5.18: Isochronous dating of a meteorite. Applying eq. (5.16), the slope defines an age of $4.55 \cdot 10^9$ years (Manhes 1982).

5.4.2 ^{87}Rb | ^{87}Sr system

^{87}Rb transforms with a half-life of $4.8 \cdot 10^{10}$ years into stable ^{87}Sr. The measurement of the two nuclides is usually made via mass spectrometry of ^{87}Rb and of ^{87}Sr/^{86}Sr, respectively. This requires a quantitative chemical separation of both elements from aliquots of the same sample. The age then follows from:

$$(^{87}\mathrm{Sr}/^{86}\mathrm{Sr})_t = (^{87}\mathrm{Sr}/^{86}\mathrm{Sr})_0 + (^{87}\mathrm{Rb}/^{86}\mathrm{Sr})_t \, (\mathrm{e}^{\lambda t} - 1) \,, \tag{5.17}$$

with λ being the transformation constant of ^{87}Rb.

While the concentration of stable ^{86}Sr is of course constant at all times, the concentration of stable ^{87}Sr at time zero is not known. It may be deduced from an isochronous plot, which includes a set of data from subsamples of the same object.

Figure 5.19 depicts the experimental data of ^{87}Sr/^{86}Sr plotted against ^{87}Rb/^{85}Sr for a gneiss sample from Greenland. The value for $(^{87}\mathrm{Sr}/^{86}\mathrm{Sr})_0$ results from the intercept of the isochronous line with the ordinate, yielding for the example depicted in Fig. 5.19 the value 0.702. Applying eq. (5.17), the slope of the isochronous line represents one age, in this case $3.66 \cdot 10^9$ years.

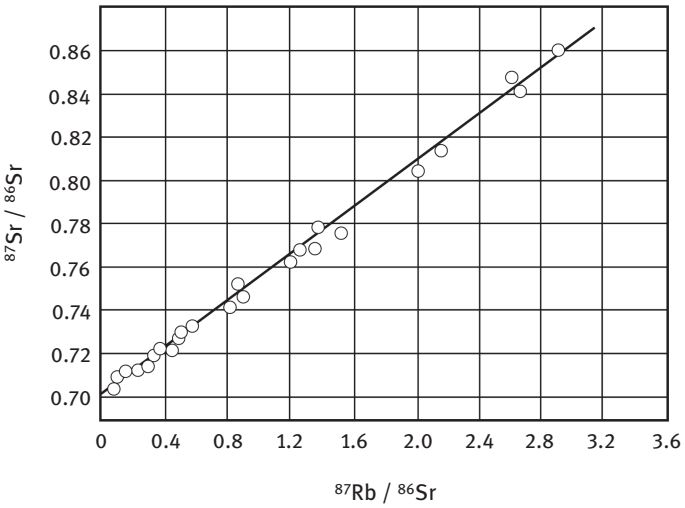

Fig. 5.19: Example of isochronous dating of several subsamples from a piece of gneiss from Greenland with the ^{87}Rb|^{87}Sr system. The slope of the line represents an age of $(3.66 \pm 0.09) \cdot 10^9$ a (Moorbath 1972).

5.4.3 ^{40}K | ^{40}Ar system

The dating is based on the 10.7 % transformation branch of ^{40}K into stable ^{40}Ar.[16] The long half-life of ^{40}K of $1.28 \cdot 10^9$ a makes this system ideal for dating igneous rocks, lunar samples or meteorites, hence, very old objects of our solar system. Argon is analyzed using a gas mass spectrometer after heating the sample to high temperatures close to the melting point. ^{40}K is usually analyzed from an aliquot of the sample using atomic mass spectrometry (AAS) or ICP-MS. As for the ^{87}Sr | ^{87}Rb system, it is very important to know the yield of the chemical separation of both elements with high accuracy. Analogous to eq. (5.17), the equation is:

$$(^{40}\mathrm{Ar}/^{36}\mathrm{Ar})_t = (^{40}\mathrm{Ar}/^{36}\mathrm{Ar})_0 + f(^{40}\mathrm{K}/^{36}\mathrm{Ar})_t\,(\mathrm{e}^{\lambda t} - 1)\,, \tag{5.18}$$

where f represents the branching ratio of 10.7 % in the transformation of ^{40}K. The ^{36}Ar concentration is constant as a function of time and therefore used as reference. The value for $(^{40}\mathrm{Ar}/^{36}\mathrm{Ar})_0$ can be determined from an isochronous plot at intercept with the ordinate at ^{40}K/^{36}Ar value at zero.

16 The more abundant branch, namely the 89.3 % of ^{40}K transforming to ^{40}Ca is of little practical use, since calcium is very abundant and the isotope ^{40}Ca has a natural abundance of 96.4 %. Hence, the very little additional ^{40}Ca formed via transformation of ^{40}K can hardly be distinguished from the vast amount of natural ^{40}Ca.

5.4.4 ^{39}Ar | ^{40}Ar system

As for the ^{87}Sr | ^{87}Rb method, the drawback of the system ^{40}K | ^{40}Ar lies in the fact that measurements have to be made on different aliquots of the sample since two different elements have to be analyzed. This can result in erroneous ages, e.g. due to heterogeneity of the sample. In recent years, a modification of the ^{40}K | ^{40}Ar method has found widespread application: the ^{39}Ar | ^{40}Ar method. The dating range is identical to the ^{40}K | ^{40}Ar method described above.

Radiogenic ^{39}Ar is a short-lived nuclide and has a half-life of 269 years. In this approach stable ^{39}K is measured indirectly via ^{39}Ar formed after neutron irradiation in a research reactor in the reaction ^{39}K(n,p)^{39}Ar. The rock samples are then heated to temperatures close to the melting point and released ^{39,40}Ar is collected and is measured via gas mass spectrometry. Typical applications include, besides Earth sciences, also age determinations of hominid fossils in Africa. In Ethiopia *Herto homonids* were dated with this method at between 160 000 and 154 000 years, making them the oldest record of modern *Homo sapiens*.

5.5 Accumulation dating with a radioactive parent and a radioactive daughter

This situation here refers to Fig. 5.2 (right part) and is met in natural transformation series. Parent and daughter nuclides are from the same transformation series, but are not the stable end products such as ^{206,207,208}Pb. Two situations exist in reality. First, at time zero the activity concentration of the daughter is zero – or negligible – (called *daughter deficient situation*, DD), but increases with time. Secondly, the activity concentration of the parent nuclide is negligibly small at all times, but the activity concentration of the daughter increases with time (*daughter excess situation*, DE).

5.5.1 ^{234}U | ^{230}Th system

These two nuclides from the ^{238}U transformation series resemble the most important example for DD-dating. The half-lives of ^{234}U and ^{230}Th are $2.455 \cdot 10^5$ years and $7.54 \cdot 10^4$ years, respectively. This limits the dating horizon to about $0.4 \cdot 10^6$ years.

The applications include solid objects formed in marine or terrestrial fluorapatites, carbonates such as corals or mollusks etc. Uranium is very soluble in water.[17] Thorium on the other hand is fully hydrolyzed at typical marine pH conditions, very insoluble and mostly adsorbed to solid particles contained in the water. These par-

17 Uranium exists in marine environment in form of $[UO_2^{2+}(CO_3)_3]^{4-}$ ionic complexes which are very soluble.

ticles sediment to the ocean floor. Therefore, the concentration of dissolved thorium in sea water is negligibly small. If objects such as e.g. stalactites in speleothems or organisms that build a shell via carbonate formation (e.g. corals) in a marine environment are formed, they will have a high concentration of uranium but are depleted in thorium. Only via radioactive transformation of uranium is thorium then formed in the solid objects. From the measurement of the activity concentration of ^{230}Th the time elapsed since formation may be deduced.

The situation refers to Fig. 5.4, being described specifically by

$$\acute{N}_{^{230}\mathrm{Th}} = \acute{N}_{^{234}\mathrm{U}}(1 - \mathrm{e}^{\lambda t}) \,. \tag{5.19}$$

λ is the transformation constant of ^{230}Th, $\acute{N}_{^{230}\mathrm{Th}}$ is the concentration at time t and $\acute{N}_{^{234}\mathrm{U}}$ is assumed to be independent of time for a given sample[18]. The reason is that ^{234}U is permanently formed via its parent ^{238}U.

5.5.2 ^{235}U | ^{231}Pa system

This couple of nuclides acts very similar to the system ^{234}U | ^{230}Th. As mentioned above, uranium is very water soluble. Protactinium, however, has a very low solubility. In its predominantly pentavalent state it is similar to the tetravalent state of thorium and very hygroscopic. The half-lives of the nuclides are for ^{231}Pa $3.276 \cdot 10^4$ years and for ^{235}U $7.038 \cdot 10^8$ years. This limits the accessible dating interval to less than about 150 000 years.

5.5.3 ^{222}Rn | ^{226}Ra system

This application represents the DD situation. In e.g. glaciofluvial[19] deposits surface water from rivers infiltrate into nearby groundwater. The infiltration velocity of such surface water into the groundwater is an important parameter for hydrological modeling. This process may be traced using the noble gas isotope ^{222}Rn ($t_{1/2} = 3.8$ d) being generated from ^{226}Ra ($t_{1/2} = 1600$ a), a member of the ^{238}U transformation series. The activity concentration of ^{222}Rn is very low in surface water due to outgassing into

18 For objects to be dated the condition of a closed system is not always met. Many samples such as bones or mollusks may experience some uranium uptake after formation. This influences the age deduced from eq. (5.12). Another possible source of error may come from the fact that activity concentration of the daughter ^{230}Th at time zero is not negligible. If e.g. the sample has some intrusions from geological materials, then this contamination contains the natural transformation series, especially ^{234,238}U. The measured ^{230}Th activity concentration then needs to be corrected for this contribution.

19 Retreating glaciers from the last ice age left many deposits in the Swiss midlands of several hundred meter thickness.

the atmosphere, hence there is no equilibrium between its precursor ^{226}Ra and ^{222}Rn. This reflects the daughter-deficient situation at time zero. This is not the case in the adjacent soil acting as bed of the groundwater. Here, secular equilibrium exists between the members of the natural transformation series. By measuring the increase of the ^{222}Rn activity concentration as a function of the distance from the river into the groundwater body, infiltration velocities may be deduced. Such an example is shown in Fig. 5.20, which yielded a mean groundwater flow velocity of 5 m per day.

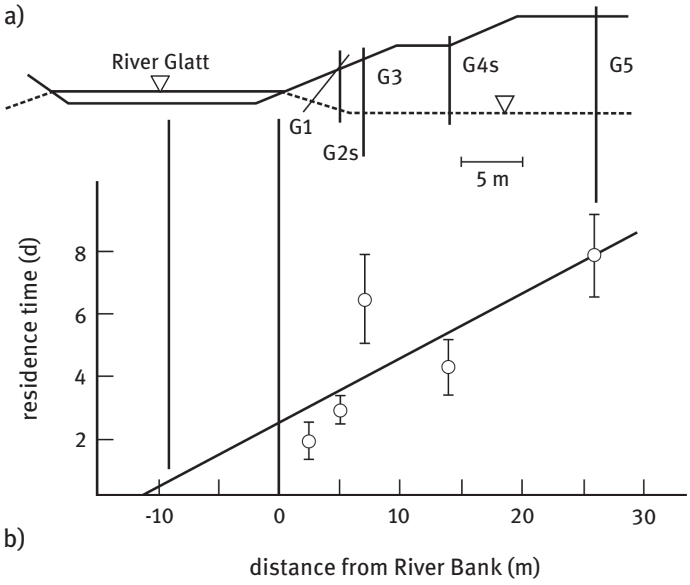

Fig. 5.20: Example of ^{222}Rn dating in hydrology. Upper part: cross section of the river (Glatt, Switzerland) with the locations of the boreholes (G1 to G5) to sample groundwater. Lower part: ^{222}Rn activity measured in water samples extracted from the boreholes (von Gunten 1995).

5.6 Dating with nuclides emitted during nuclear weapons testing and nuclear accidents

On several occasions, manmade radionuclides have been emitted into the environment. These events may be used as dating horizons if stored in environmental archives. One of the most important emission sources were the aboveground[20] nuclear weapons testing series conducted by USA and Soviet Union. Many radionuclides such as fission products, bomb material or secondary products from interaction with

20 "Aboveground" nuclear tests in contrast to "underground" tests.

neutrons were emitted into the atmosphere. In the late 1950s such tests were performed by USA in the Bikini Atoll that led to activation of sea-salt particles contained in the plume of the explosion. Figure 5.21 depicts some typical debris isolated from the ice of a glacier in Switzerland. It includes material from the bomb itself such as ^{239}Pu ($t½ = 2.41 \cdot 10^5$ a), products formed in nuclear fission such as ^{137}Cs ($t½ = 30.2$ a), activated (by the enormous intensity of neutrons) sea-salt aerosol particles such as ^{36}Cl ($t½ = 3.0 \cdot 10^6$ a) from the early tests over the Bikini Atoll, and tritium ($t½ = 12.3$ a), which was formed in the hydrogen bombs also via interaction with neutrons. These nuclides were largely injected into the stratosphere from where they returned into the troposphere within several years. For the fission product ^{137}Cs, the emission into the European atmosphere caused by the Chernobyl accident in April 1986 is also observed. In this case, however, the transport occurred within the troposphere. These stratigraphic radioactive horizons are also often found in other archives such as e.g. lake sediments (see ^{137}Cs in Fig. 5.11 in Section 5.3.2).

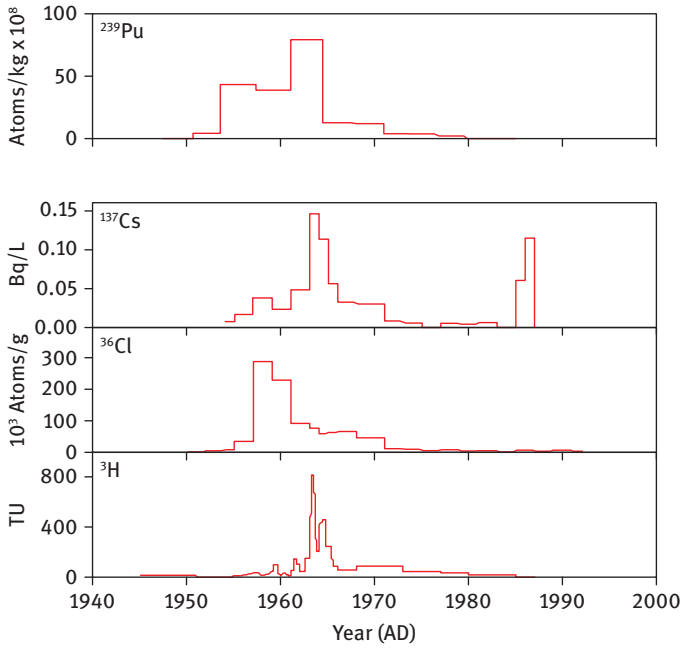

Fig. 5.21: Radionuclides detected in ice cores from glaciers in Siberia (Belukha, Russia, ^{239}Pu) and from the Alps (Grenzgletscher, Switzerland, ^{137}Cs, ^{36}Cl, ^{3}H) that can be assigned to nuclear weapons testing in the late 1950s and early 1960s and to the Chernobyl accident in 1986 (activities in units of Bq/l or TU (1 TU = 0.18 mBq/l)) (Olivier 2004 (upper part); Eichler 2000 (lower part)).

5.7 Fission tracks

^{238}U is ubiquitous in nature. The average concentration in the Earth's crust is 5 ppm. ^{238}U mostly transforms via α-emission and to a much lesser extent by spontaneous fission (sf).[21] Primary fission fragments have very high kinetic energies and therefore damage the surrounding matrix leading to tracks. These so-called latent fission tracks have a length of typically 10 to 20 µm. These tracks become visible by chemical etching, cf. Chapter 2, and can be counted using a microscope. From the number of observed fission tracks and knowing the concentration of ^{238}U, the age may be inferred based on the known half-life of ^{238}U. Best suited for determination of the ^{238}U concentration is to measure ^{235}U via thermal neutron induced fission. ^{235}U has an abundance in natural uranium of 0.7 %. The procedure then goes as follows: first the sample is etched and the number of fission tracks from ^{238}U is determined. Then the sample is irradiated at a research reactor with thermal neutrons that initiate induced fission (if) of ^{235}U. The additionally formed fission tracks are again etched and counted. From the added number of new fission tracks and the natural abundance the concentration of ^{238}U can be inferred. This leads to the age Δt of a sample according to:

$$\Delta t = \frac{1}{\lambda}\,(^{238}\mathrm{U})\,\ln\left\{1 + \left[1.61 \cdot 10^{4}\,\frac{D(\mathrm{sf})}{D(\mathrm{n,if})}\,\delta_{(\mathrm{n,if})}\,\Phi_{\mathrm{n}}\,t_{\mathrm{irr}}\right]\right\} \tag{5.20}$$

with D(sf) and D(n,if) being the fission track densities from ^{238}U and from ^{235}U in the sample, respectively, $\delta_{(\mathrm{n,if})}$ the cross section for thermal neutron induced fission of ^{235}U (= $5.86 \cdot 10^{-22}$ cm^2), Φ_{n} the flux of thermal neutrons in n cm^{-2} s^{-1}, and t_{irr} the irradiation time.

One major drawback in fission track dating is annealing. In the course of time some tracks may fade away due to thermal processes or due to ion diffusion. This may lead to narrower and shorter tracks. As a consequence, underestimated ages may result. Annealing depends greatly on the material. Zircon or titanite are influenced very little by annealing, while e.g. apatite is much less stable.

Fission track dating has been successfully applied in dating of tephra and obsidian from volcanic eruptions for up to several hundred millennia. It was e.g. possible to date tephra in the lee of the Andes (Rio Grande Valley) to have an age of 225 000 ± 25 000 years (Espizua 2002).

5.8 Thermoluminescence dating

Soil or rock usually contain radionuclides such as isotopes of uranium, thorium, potassium etc. The emitted radiation in the material forms ion-electron pairs. Often, these electrons are trapped in structural defects of crystal lattices and can then be

21 Cf. Chapter 10 in Vol. I. The probability for sf in ^{238}U is only $4.5 \cdot 10^{-5}$ %.

released in the laboratory via controlled heating. As a consequence, light signals are observed. Loosely bound electrons lead to light pulses at heating temperature of about 100 °C, while highly bound electrons need heating temperatures in excess of 500 °C to ignite light emission. Photon detection is usually plotted against the heating temperature (glow curve), in which peaks reflect the various electron trap configurations in the material. It turned out that high temperature thermoluminescence is proportional to the irradiation dose of the material. The age of a sample can then be determined from the known natural dose per year in the sample. However, the energy deposited in the material is strongly dependent on the nature of radioactivity: α-particles have a high LET (linear energy transfer) value, but on a short distance of typically some 20 to 50 µm, while β-particles are stopped with a much lower LET value within a range of several mm. Gamma rays, finally, have very few interactions and as a consequence very long stopping ranges. This means that for each type of irradiation a calibration is required for the dose to light emission relationship. In addition, the linearity in this relationship is limited: for e.g. quartz, saturation of the light emission is observed at 100–500 Gray (Gy), while calcite saturates at a much higher dose of about 3 kGy. To conclude, thermoluminescence dating should be applied with a certain degree of caution and, if possible, verified with some other dating options. In real applications, thermoluminescence dating turned out to be suited for the time window between ^{14}C and $^{40}K\,|\,^{40}Ar$ dating.

5.9 Outlook

Nuclear dating has found widespread application in many fields of science. The time range that may be analyzed is huge: it covers hours to billions of years. However, nuclear dating very much depends on the known accuracy of the half-life of the radionuclides involved. Some environmental radionuclides still have poorly known half-lives that need further improvement. One example mentioned in this chapter is ^{32}Si. Published values range from about 100 to 170 years, which prevents application of this nuclide for dating purposes. Another example is ^{60}Fe (not mentioned in this chapter). Its half-life was published to be $1.5 \cdot 10^6$ a. Recently, it was re-measured and the new value is now $2.6 \cdot 10^6$ a (Rugel 2009).

One drawback in nuclear dating is the analytical challenge: usually the samples to be dated contain only tiny amounts of the radionuclide that serves as a “clock” to determine the age. Earlier, the determination of such radionuclides occurred mostly via radiometric techniques. Recently, thanks to technological progress, mass spectrometry has gained increased importance due to considerably improved sensitivity. This made it possible to measure e.g. radionuclides with half-lives greater than about 100 years in environmental samples with accelerator mass spectrometry (AMS) down to a level of less than 10^6 atoms.

The "workhorse" in nuclear dating is still radiocarbon, ^{14}C. This situation will probably remain so in the future, simply because many objects to be analyzed contain carbon. Hence, many laboratories have recently ordered miniaturized AMS devices, now available on the market, that are fully dedicated to measure radiocarbon with supreme sensitivity and accuracy.

5.10 References

Appleby PG. The Holocene. 2008, 18, 1, 83–93.

Balco G, Stone JO, Lifton NA, Dunai TJ. A complete and easily accessible means of calculating surface exposure ages or erosion rates from ^{10}Be and ^{26}Al measurements. Quaternary Geochronology, 2008, 3, 174–195.

Bonani G, Ivy SD, Hajdas I, Niklaus TR, Suter M. AMS ^{14}C age determinations of tissue, bone and grass samples from the Ötztal Ice Man. Radiocarbon, 1994, 36, 247–250.

Eichler A, Schwikowski M, Gäggeler HW, Furrer V, Synal HA, Beer J, Saurer M, Funk M. Glaciochemical dating of an ice core from upper Grenzgletscher (4200 m asl). J Glaciol 2000, 46, 507–515.

Erten HN, von Gunten HR, Sturm M. Dating of sediments from Lake Zürich (Switzerland) with ^{210}Pb and ^{137}Cs. Schweiz Z Hydrol 1985, 47, 5–11.

Espizua LE, Bigazzi G, Junes PJ, Hadler JC, Osorio AM. Fission-track dating of a tephra layer related to Poti-Malal and Seguro drifts in the Rio Grande basin, Mendoza, Argentina. J Quaternary Sciences 2002, 17, 781–788.

Gäggeler H, von Gunten HR, Nyffeler U. Determination of ^{210}Pb in lake sediments and in air samples by direct gamma-ray measurements. Earth and Planetary Science Lett 1976, 33, 119–121.

Gäggeler HW, von Gunten HR, Rössler E, Oeschger H, Schotterer U. ^{210}Pb-dating of cold Alpine firn/ice cores from Colle Gnifetti, Switzerland. J Glaciol 1983, 29, 101, 165–177.

von Gunten HR. Radioactivity: A tool to explore the past. Radiochim Acta 1995, 70/71, 305–316.

Friedländer G, Kennedy JW, Macias ES, Miller JM. Nuclear and radiochemistry. 3rd edition, Wiley, 1981.

Heijnis H. Uranium/Thorium dating of late pleistocene peat deposits in N.W. Europe. The Netherlands, Rijksuniversiteit Groningen, 1995.

Manhes G. Thèse, Univ. de Paris VII, 1982 (cited in von Gunten, 1995).

Moorbath S, O'Nions RK, Pankhurst RJ, Gale NH, McGregor VR. Further rubidium-strontium age determinations on the very early Precambrian rocks of the Godthaab District, West Greenland. Nature Phys. Sci. 1972, 240, 78–82.

Morgenstern U, Geyh MA, Kudrass HR, Ditchburn RG, Graham IJ. ^{32}Si dating of marine sediments from Bangladesh. Radiocarbon 2001, 43, 909–916.

Olivier S, Bajo S, Fifield KL, Gäggeler HW, Papina T, Santschi PH, Schotterer U, Schwikowski M, Wacker L. Plutonium from global fallout recorded in an ice core from Belukha Glacier, Siberian Altai. Env Sci Techn 2004, 38, 6507–6512.

Rugel G, Faestermann T, Knie K, Korschinek G, Poutivtsev M, Schumann D, Kivel N, Günther-Leopold I, Weinreich R, Wohlmuther M. New measurement of the ^{60}Fe half-life. Phys Rev Lett 2009, 072502/1–072502/4.

Stuiver M, Earson GW, Braziunas T. Radiocarbon age calibration of marine samples back to 9,000 CAL yr BP. Radiocarbon 1986, 28, 980–1021.